Application of Accelerated Carbonation and water curing for development of superplasticed Self Compacting Concrete

S.O. Odeyemi[1*], A.I. Amoo[2], R. Abdulwahab[3], A.A. Adedeji[4]
[1,2,3]Department of Civil and Environmental Engineering,
Kwara State University.
[4]Department of Civil Engineering, University of Ilorin
[1]samson.odeyemi@kwasu.edu.ng; [2]amooafusat1@gmail.com;
[3]abdulwahab.rasheed@kwasu.edu.ng; [4]aaadeji@unilorin.edu.ng

Abstract

The growing shortage of raw materials coupled with the vital requirement to shield the ecosystem from pollution has heightened the need to develop novel construction materials from agricultural wastes. Therefore, the goal of this work was to determine the properties of GCHA blended Self Compacting Concrete (SCC) using Accelerated Carbonation Curing (ACC) and water curing methods. Portland limestone cement, Guinea Corn Husk Ash (GCHA), sand, water and granite dust were tested for fineness, coarseness, specific gravity before being used to produce the concrete samples. The concrete was also investigated for its flowability parameters. Also, Scanning Electronic Microscopy (SEM), Energy Dispersive X-Ray Fluorescence Spectrometer (EDXRF, X-Ray Diffraction (XRD) were carried out to determine the properties of the GCHA. The mix ratios for the self-compacting concrete were developed and optimized to obtain an optimal compressive strength. The optimum combinations of percentage of GCHA and cement in ACC that gave a compressive strength of 21.369 N/mm^2 in 56 days are 25 % and 412.5 kg/m^3 respectively. The flowability properties such as slump flow T50 was obtained at 5 seconds, slump flow was 690 mm, L-box was 0.88mm and V-funnel was 6 seconds for ACC. The optimum combinations of percentage of GCHA and cement in WC that gave a compressive strength of 19.6274 N/mm^2 in 56 days are 25 % and 412.5 kg/m^3 respectively. The flowability properties such as slump flow T50 was obtained at 6 seconds, slump flow was 700 mm, L-box was 0.81mm and V-funnel was 5 seconds for WC. Therefore, the optimal combinations for ACC and WC can be used in reinforced concrete production.

Keywords

Accelerated carbonation curing, central composite design, durability, flow parameter, guinea corn husk ash, water curing

1. Introduction

The three basic requisites of humans are food, clothing, and shelter. To provide shelter, the paramount thing needed is concrete. Hence, concrete is the second most selling product just after water (Dharmesh *et al.*, 2014). Concrete is most versatile man-made construction material. It can be shaped into variety of forms. It contains aggregates held together by cement paste in a specific mix design depending on the required strength. The water to cement ratio (w/c) plays a major part in determining the compressive strength of concrete (C. A. Fapohunda, Famodimu, Adigo, & Jeje, 2020). Cement is considered as a hydraulic binder because it hardens by reacting with water to a product that is insoluble in water. The types and proportions of the constituents of influence both the hard and fresh properties of the concrete (Bhagat, Dawda, Goyal, Navneet, & Panchal, 2014).

SCC is considered as an innovative discovery in the history of concrete technology since it can be compacted under its own weight without vibration. It can also fill gaps in clogged reinforcements or geometrically intricate structures without bleeding or segregating. This implies that SCC is a perfect concrete material that fulfills the basic requirements of passing ability, filling ability, and segregation resistance. The goal of applying SCC for construction is to have a concrete with more durability and reliability, higher performance, improved strength, and faster construction period (Kashani & Ngo, 2020; Su, Hsu, & Chai, 2001). For self-compacting concrete, it is generally important to use super-plasticizers and some volume of admixtures such as fly ash, silica fume, glass filler, corn cob ash, etc. Super-plasticizer improves deformability and the decrease in w/c and reduction in the volume of aggregates leads to an increase in segregation resistance in SCC (Kashani & Ngo, 2020). Exploring a way of reducing the quantity of cement in concrete is an efficient means of bringing down cost of concrete production because cement is the costliest component of concrete.

Moreover, the mineral admixtures have the capacity of reducing the permeability of concrete while improving its particle packing structure and durability. Industrial wastes such as fly ash, limestone powder, and granulated blast furnace slag are largely adopted as mineral admixtures in SCC (Pathak & Siddique, 2012). In so doing, there is an improvement in the workability of SCC and the quantity of agricultural by-products used can be increased. Aside the economic benefits, the incorporation of agricultural by-products in

concrete helps to reduce environmental pollution (Aggarwal, Siddique, Aggarwal, & Gupta, 2008; Su et al., 2001).

The constant hike in the price of cement, a binder in the production of sandcrete blocks, mortar, concrete, and lancrete bricks has necessitated the search for alternatives. Along with cost, the emission of CO_2 (a major cause for global warming), high energy demand, and the depletion of limestone deposits are some demerits associated with the production of cement (Ehikhuenmen, Igba, Balogun, & Oyebisi, 2019; He, Shi, Tu, Poon, & Zhang, 2016). The quantity of CO_2 discharged into the atmosphere when cement is produced poses a great threat to existence of humanity and affects the ecology negatively (Adeyanju & Okeke, 2019). Much published research on finding alternatives to cement has focused on the partial replacement of cement with pozzolans (siliceous material). A combination of Portland cement and pozzolanic materials is known as pozzolanic cements (McCarthy & Dyer, 2019).

In the third world countries, the most common materials used as cement replacement without economic consequences are agro based wastes. Prominent among them are Bambara groundnut shell ash (BGSA), Acha husk ash (AHA), Groundnut husk ash (GHA), Bone powder ash (BPA), Wood Ash (WA) and Rice husk ash (RHA). They also include ashes from the calcination of bagasse, dried banana leaves, periwinkle shell ash (PSA), bamboo leaves, and sawdust. Some of the advantages derived from using agro-wastes as partial replacement of cement are waste management at minimal cost, reduced production cost per tonne compared to cement, increased economic base of farmers when the wastes are utilized and reduced pollution by the agro wastes. These advantages thereby encourage production by farmers, reduction in CO_2 emission and preservation of limestone deposits.

Guinea corn is typically harvested and milled manually for food, leaving a large chunk of residue becoming wastes on the farms. These are often flared off when preparing for subsequent farming seasons. GCHA is a product of calcining guinea corn husk and the chemical composition of GCHA showed that it is qualified to be classified as pozzolana (Ndububa & Yakubu, 2015; Odeyemi, Anifowose, Abdulwahab, & Oduoye, 2020). Since GCHA is abundantly available coupled with its suitability as pozzolana, it is imperative to investigate optimal ways of using it to mitigate its contribution to environmental pollution and hazard.

Hence, this research aims at studying the optimal use of GCHA as a fractional substitute for cement in SCC using Central Composite Design (CCD), a Response Surface Method (RSM) tool in design expert software package. The objective function is the compressive strength of the concrete while maximizing the use of GCHA.

2. Materials and Methods

2.1 Materials

All the resources used for this experiment were procured from Ilorin, Nigeria. The British standard was used in conducting the experiments. The materials for this study include Sand, Cement, GCHA, superplasticizer, viscosity modifying agent and water.

GCHA was sourced from Alapa, University of Ilorin and Ore village. Samples of the Guinea Corn Husk (GCH) collected were calcined at 650℃ using thermolyne furnace at Institute of Technology of the Kwara State Polytechnic as recommended by Odeyemi *et al.* (2020). The Guinea corn husk was calcined at 650℃ to obtain the desired chemical composition of the GCHA required for SCC (Bello, Abdus-Salam, & Adekola, 2018). The ash was allowed to cool then ground and sieved to a fine texture by allowing it to pass through sieve no 75 µm. Chemical analysis tests were carried out to ascertain its chemical properties.

Portland Limestone Cement (PLC) of grade 42.5R conforming to BS EN 12620:2002+A1:2008 (2008) was used in this study. Laboratory tests such as normal consistency, soundness and finesse were carried out following the British standard. Sharp sand obtained from Asa River in Ilorin was adopted as fine aggregate. This was tested for its fineness modulus specific gravity, sieve analysis, water absorption, and particle size distribution in accordance to BS EN 933-1 (2012).

Crushed stone (granite) was utilized as coarse aggregate. The coarse aggregate was sieved and the particle-size distribution ranges from 4.75 mm to 10 mm. The Specific gravity, aggregate crushing value, and Water absorption of the coarse aggregate were duly tested. Polycarboxylic ether based High Range Water Reducing (HRWR) admixture with inbuilt Viscosity Modified Admixture (VMA) with a brand name of BETOCRETE- F4 (FM) was used in

this work as superplasticizer. It was gotten from Advance Concrete Technologies LTD., Abuja, Nigeria.

The water used for mixing the concrete was gotten from the Concrete Laboratory of the Civil Engineering Department of the Kwara State University. The pH of this water was measured using a portable pH meter with Model number S-903. It was investigated to confirm that it does not contain any deleterious material that might distort the reaction between the GCHA and the compounds of lime in cement.

2.2 Methods

2.2.1 Fineness Test on PLC and GCHA

The Fineness of PLC and GCHA were obtained by using a 90 microns BS sieve. The weight of an empty pan was taken and recorded. A spatula was used to add one hundred (100) grams of cement sample to the tray and both weights were recorded. For a period of 15 minutes, the cement in the sieve was vibrated vertically and in circular motions. The weight of the residue on the sieve was recorded. The fineness was obtained using Equation 1.

$$\textbf{Fineness} = \frac{\textbf{Percentage of Sample Re tained on Sieve}}{\textbf{100}} \quad (1)$$

2.2.2 Fineness Modulus Test

The fineness modulus was conducted as recommended in BS EN 933-1 (2012). It was obtained from Equation 2 by summing up the cumulative percentage of aggregates left on each sieve and dividing the result by the weight of the sample. The test sample was dried in an oven at a temperature of 110±5 ℃, weighed and sieved in an electric sieve shaker with a set of BS sieves. After sieving, the weight was recorded. The cumulative weight going through each sieve was calculated as a fraction of the total weight of the sample.

$$\textbf{Fineness Modulus} = \frac{\textbf{Total Cummulative \% Retained}}{\textbf{100}} \quad (2)$$

2.2.3 Specific Gravity Test

The specific gravity of the samples was conducted as specified in BS 1377:2 (2018). Unwanted particles were removed from the samples. An empty bottle was weighed, and the weight designated as W_1. Sample was filled into the bottle, weighed, and recorded as W_2. Distilled water was filled into a bottle containing the sample up to a point that has been marked. Entrapped air and

surface bubbles were removed by shaking the bottle vigorously before taking the weight. This weight was recorded as W_3. After this, the bottle was emptied and dried in an oven. The dry bottle was subsequently filled with distilled water to the marked point, weighed and recorded as W_4. Equation 3 was then used to get the specific gravity.

$$\textbf{specific gravity} = \frac{\mathbf{W_2 - W_1}}{(\mathbf{W_4 - W_1}) - (\mathbf{W_3 - W_2})}. \quad (3)$$

2.2.4 Normal consistency for cement

To perform the normal consistency test, 300g of cement was put in a mixing plate. A crater was created at the centre in which measured quantity of water (to start with 25 % of water: 75ml) was added. After 30 seconds, the material was thoroughly turned for one minute. The resulting mixture was introduced into a ball and tossed to and fro about six times from one hand to the other hand. With the ball resting in the palm of one hand, the materials were pressed into the mould through its larger end and then smoothen off the top of the paste with a trowel. Afterwards, the moulds were placed with its bigger end on a glass plate and smoothen off the top of the paste at the small end. Thereafter, the mould on the glass plate was placed in the Vicat apparatus. The scale was then set to zero bringing the end of the plunger in touch with the paste surface and then released. The penetration was recorded. The experiment was repeated with pastes containing different percentages of water. The quantity of water (normal consistency, mm) mixed is stated as a percentage by weight of the cement as given in Equation 4.

$$\text{Normal Consistency} = \frac{\text{sum of the plunger}'\text{s penetration of sample 1 and 2}}{2} \quad (4)$$

2.2.5 Soundness Test

To carry out this test standard consistency of cement was needed. Cement of 400 g was used for this experiment. The cement paste was thoroughly agitated and poured into Le-Chatelier's mould. The clean upper surface of paste in the mould was adjusted to smoothness after which a small weight was positioned on the cover plate. The mould was immediately inserted in the water for 24 hours at a temperature of 27℃. After this, the mould was taken out from the water. The range between the indicator points was determined and taken as Reading 1. Furthermore, this mould was again introduced in the boiling water for 3 hrs. Afterwards, the mould was taken

out of the boiling water and allowed to cool to ambient temperature. The gap (distance) between the indicators point was also recorded as Reading 2. From the recorded values Equation 5 was used to calculate the soundness of cement.

$$\text{Soundness of cement} = (\text{Reading 2}) - (\text{Reading 1}) \quad (5)$$

2.2.6 Setting Time Test

Having determined the normal consistency of the sample, 1 mm square needle was fixed at the lower end of the Vicat apparatus and allowed to get in touch with the surface of the paste. It was read by the scale and then released. The penetration was noted. The experiment was repeated until the paste had stiffened enough for the needle to pierce no further than a distance approximately 5-7 mm from the end of the mould. The time between when water was introduced to the cement and the time when the needle does not penetrate beyond 5 from the bottom part of the mould was recorded. The time when the needle could only make an indentation on the surface of the paste was also noted. These values were used to determine the setting times as shown in Equations 6a and 6b.

$$\text{Initial setting time (IST)} = T_2 - T_1 \quad (6a)$$

$$\text{Final setting time (FST)} = T_3 - T_1 \quad (6b)$$

Where T_1 = Time of penetration to the bottom of the mould; T_2 = Time when the needle could not go beyond 5 mm from the bottom of the mould; T_3 = Time when the needle could only make an indent at the surface of the mortar.

2.2.7 Water absorption test

Aggregate of 2 kg was utilized for the experiment. The aggregate was washed and put in a wire basket. This basket was then immersed in water at 27 ℃. The entrapped air was removed from the sample just after immersion by lifting the basket 25 mm above the bottom of the tank. It was then dropped about 25 times, each drop per second. The immersion was allowed for 24 hrs after which the basket and aggregate were weighed while dipped in the water. The basket containing the aggregates were taken out of the water and dried with a piece of cloth. The surface dried aggregate was weighed and placed in a tray for heating at 100 ℃ for 24 hours in an oven. It was then cooled in an airtight container and weighed. The water absorption (%) was calculated using Equation 7.

$$\text{Water Absorption (\%)} = \frac{(W_1 - W_2)}{W_2} \text{x } 100. \quad (7)$$

Where W_1 = Weight of saturated aggregates in air (g) and W_2 = Weight of oven dry aggregates in air (g).

2.2.8 Sieve analysis Test

This test was conducted on both the fine and coarse aggregates to determine their particle size distribution (whether well graded or gap graded) following the procedure found in BS ISO 3310-2 (2013). The aggregates were oven dried at 105 ℃ for hours. Set of BS sieves were utilized for the sieving operation. The size of the sieve used for the fine aggregate ranges from 0.075 mm to 2.36 mm. The size of sieves for the coarse aggregate ranges from 4.76 mm to 31.75 mm. A lid was placed at the bottom of the sieves in both cases. The particle size distribution curve was computed after the sieving operation.

2.2.9 Aggregate crushing value (ACV)

Aggregates were placed on a plate and weighed (W). The aggregates were compacted in 3 layers with each layer subjected to 25 strokes using a steel rod. The compacted aggregate was weighed and designated as W_1. The top of the aggregate was cautiously leveled, and a plunger was placed at 90^0 to the surface of the mould. Thereafter, the aggregate with plunger was placed in compression testing machine. Load of 40,000 kg was applied for 10 minutes. After 10 minutes, the aggregates were sieved with 2.36 mm BS sieve (loss was avoided to ensure accurate reading). Fractions that pass through the sieve was then weighed (W_2). The ACV was calculated as using Equation 8

$$\text{ACV} = \frac{W_2 \text{ x } 100}{W_1 - W}. \quad (8)$$

Where W_2= weight of fraction passing through the appropriate sieve; W_1- W = weight of surface dry sample.

2.2.10 Design Experiment

The European Federation for Specialist Construction Chemicals and Concrete Systems (EFNARC) mix design procedure was adopted for mix proportioning of the SCC. Trial mixes with variable percentages of GCHA, ranging from 0% to 25% (0 – 125 kg/m^3) of GCHA, cement 75 % - 100%

(375 – 500 kg/m^3) were utilized for the study. All other material were kept constant i.e. water to cement ratio of 0.45, sand 960 kg/m^3, granite dust 100 kg/m^3, crushed granite of 813 kg/m^3 and super-plasticizer 1.5 L/100kg of cement as recommended by Akinpelu *et al.* (2019) for Grade 20 SCC concrete. Table 1 reveals the boundary coded levels for materials used in this study. The boundary condition for each parameter was imputed using CCD, a method of RSM in Design Expert Software. The responses from the combinations of experiment are the flowability parameters (slump flow, slump height, L-box and V-funnel results) and compressive strength.

2.2.11 Setup for ACC

Accelerated Carbonation Curing (ACC) chamber for the curing of the samples concrete was constructed for this experimental study. The total length, width and height were 1.0m X 1.0m X 1.0m while the inner length, width and height of the ACC chamber that could contain 60 cubes (each of $0.1m^3$) were 0.9m by 0.9m by 1m respectively.

Table 1 The experimental variables and levels used for concrete mixtures

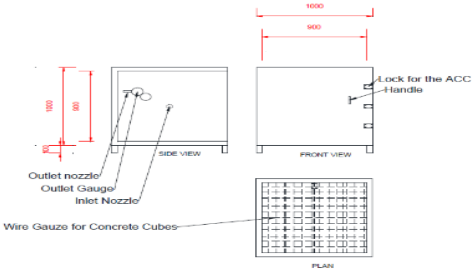
Materials	Units	Coded Levels	
		-1	**+1**
GCHA	%	0	25
Water to cement ratio	-	0.45	
Cement	kg/m^3	375	500
Super-plasticizer	L/100kg		1.5
Sharp sand	kg/m^3		960
Granite dust	kg/m^3		100
Crushed granite	kg/m^3		813

The inner part was built in three layers so that 20 cubes could be arranged. Galvanized plate of 0.6mm thickness was used for the inner construction which helped to prevent the inner corrosion of the chamber while the outer layer thickness was 0.7mm black plate. FEV COL pur adhesive material was used as a moisture curing polyurethane adhesive, which served as glue that bond both the outer layer and the inner layer plate together. There were two valves that regulate the inflow and out flow of CO_2 gas, one on top of Cylinder gauge and the other one at the outlet of chamber. A door was installed for accessing the chamber for the purpose of inserting and removing the cube samples.

There are three (3) holes in the wall of the chamber. One of them is the inlet hole which was connected to the CO_2 cylinder. The second hole was linked to a pressure gauge to monitor and control the pressure in the ACC chamber. The last outlet was inserted to remove the CO_2 gas from the chamber after the curing operation. 4 mm steel plate was utilized for the fabrication of the chamber to ensure its operational safety and efficiency. The snapshot of the chamber and its orthographic view is shown in Figure 1.



Picture of the chamber



Plan of the chamber

Figure 1: Accelerated carbonation chamber

2.2.12 Curing process

A total of 234 concrete cubes were cast. 117 were cured by immersion in water while the remaining 117 were cured in ACC. The chamber for the ACC curing was tightly closed to avoid escape of the CO_2 gas and to allowed the gas circulate within the chamber for ten (10) hours as recommended by Assaggaf et al. (2019). Samples of the cubes were taken out of the chamber after 10 hours to determine their performance in compressive strength. The samples cured in water were immersed for a maximum number of 56 days. The compressive strength of each concrete sample was determined after 7, 28 and 56 days of curing.

2.2.13 Compressive Strength Test

The compressive strength test was conducted as spelt out in BS EN 12390-3 (2019). The samples were brought out of their curing chambers and tested at 7, 28 and 56 days of curing using a compression testing machine of 1500 kN

capacity. For each run of experiment, 3 cubes were crushed to obtain an average strength.

2.2.14 Durability Test

The samples were evaluated for their durability using two test procedures reported in Fapohunda *et al.* (2020). These procedures are the sorptivity test and the coefficient of water absorption test.

2.2.15 Coefficient of water absorption test

This test measures the rate at which water is taken in by dry concrete samples in 1 hour determined. Preconditioning of the samples was performed by drying them for three (3) days in an oven at 105 ℃. During this period a constant weight of the samples was achieved. The samples were then removed from the oven and allowed to cool in an airtight container for another three days. Since it was required for water to flow in a direction in this test, all sides except one of the concrete samples were coated with silicone sealant. Then, the samples were partially immersed in a vertical position to a depth of 5 mm at one end, while the remaining sides were exposed to the ambient air. The volume of water absorbed by the concrete samples in the first 60 minutes was determined. Equation 9 was considered in calculating the Coefficient of water absorption (K_a) for the concrete specimens after 56 days curing.

$$K_a = [\frac{Q}{A}]^2 x \frac{1}{t} \quad (9)$$

Where t = duration curing, A= Area of concrete, Q = Quantity of water absorbed.

2.2.16 Sorptivity test

The tests were carried out at selected times ranging from 0 to 120 minutes. At the times under consideration, the samples were taken from water and excess water dried off using a damp paper towel before weighing the sample. The samples were then placed back in water until another selected time. The gain in mass per unit area over the density of water was plotted versus the square root of the elapsed time. The cumulative water absorption (per unit area of the inflow surface) is thought to increase as the square root of elapsed time (t), increases. The slope of the line of best fit of these points was taken as the

sorptivity value. Equation 10 was adopted in determining the sorptivity values of the blended concrete specimens at 7, 28 and 56 days of curing.

$$i = \frac{s}{\sqrt{t}}. \quad (10)$$

Where i = sorptivity; s = slope and t = time.

2.2.17 Characterizations

X-Ray Diffraction (XRD) on GCHA

The XRD analysis was carried out at NASENI Co Ex, Akure, Ondo State. The equipment (GBC Difftech XRD-MMA) with a model number of EMMA014 and CuKα radiation of λ=1.54060 Å was utilized. It has its design specifications at maximum power of 3.0 kW, voltage ranging from 0 – 60 kV and ampere ranging from 0 – 80mA. Its long-term stability is 0.01 % over 8 hours of performance. Its ripple displays at 0.003% rms. To achieve a high-resolution scanning, a tripod that allows very high precision height adjustment was mounted. The radius varies from 175 mm out to 250 mm ($K\alpha_1$ and $K\alpha_2$ peaks completely separated at 80 deg with CuKα). The scanning speed with full multi-pass averaging 0.0002º/min to 60 º/min. The range of 2θ = 0 to 70 with scanning step size of 0.002º was used to determine the chemical phase and the crystalline structure of the GCHA.

Energy Dispersive X-Ray Fluorescence Spectrometer (EDXRF)

The EDXRF analysis was carried out at NASENI Co Ex, Akure, Ondo State. The Skyray EDXRF analyzer (EDX 3600B) was used to determine both the elemental and oxides compositions of the GCHA. The equipment was designed with the following specifications: analyzable element ranging from $11^{Na(sodium)} - 92^{U\ (uranium)}$; analyzable element content ranges dynamically from ppm- level to nearly 100 percent; test time (60 sec- 200 sec with extra 50 sec if vacuum requires); inside dimension of sample chamber of 320mm (diam) x 180 mm (height); maximum voltage of 50kV; dimension of spectrometer is 608 mm long by 650 mm wide by 466 mm high.

To test the sample, the voltage of the equipment was regulated to achieve the required power from the x-ray source. Standardization of the XRD software on the computer system was done using a pure silicon sample. Thereafter, the non-homogeneous sample (GCHA) was ground to a homogeneous size before loading into the equipment's sample holder. The run parameters such as end angle, start angle, speed and step size were selected before scanning

the sample. The equipment analyzed the samples and compared them to the XRD standard reference.

2.2.18 Scanning Electronic Microscopy (SEM)

The SEM analysis was carried out at Material Laboratory of the Department of Material Science and Engineering, Kwara State University, Malete. The SEM ASPEX 3020 was used to investigate the surface morphological structure of GCHA. In order to test the sample, electrons were fired into the sealed vacuum chamber that holds the sample. The sample was gold plated using a balzer's sputtering device, before placing it under a microscope. An electromagnetic coil in the equipment acts like a lens by bringing the electron beam to a very precise focus. Another coil at the lower part of the equipment steers the electron beam from one side to another in order to scan all areas of the sample. The electrons got in contact with the surface of the sample before bouncing off it. A detector then records the scattered electrons and converts them to an image. The SEM displayed the image of the sample at different magnifications of 250, 500, 750 and 1000 on a mode of 16 kV accelerating voltage.

3. Results and Discussions

3.1 Results for Materials used in casting SCC

3.1.1 Determination of Fineness of Cement by Sieving Method

Table 2 shows the fineness of cement. This result indicates that the cement is homogenous and fit for concrete production.

Table 2 Description of the fineness of cement by sieving method

Description	I	II
Weight of cement sample(g)	100	100
Weight of residue of cement(g)	1	2
% of fineness of cement (%)	1	2
Average % of fineness of cement (%)	1.5	

3.1.2 Sieve Analysis Results for Sharp sand

The fine modulus obtained from the sieve analysis was 2.869 % which falls within the range (2.2 % -3.2%) for fine aggregates. Similar results were obtained by Odeyemi *et al.* (2020b) when they determined the fine aggregate of sharp sand used in the casting of concrete containing GCHA as an additive. Figure 2 confirms the size of the sand particles used in the research

as the grain diameter were found to between 0.080 mm to 2.5 mm with most grains falling in the fine range of particle distribution.

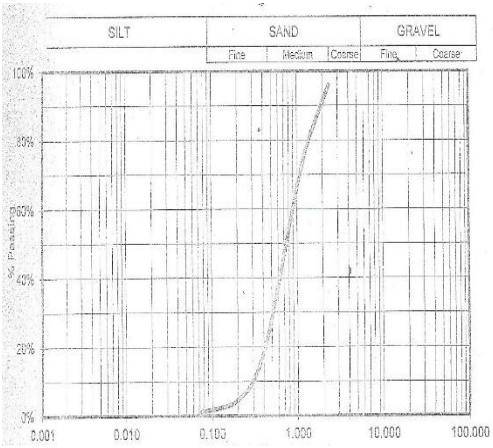


Figure 2: Particle size analysis for sharp san

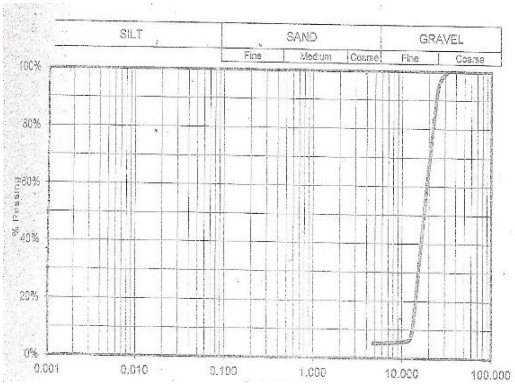


Figure 3: Particle size analysis for granite

3.1.3 Sieve Analysis Result for Granite

Table 3 shows the sieve analysis for coarse aggregates (granite) obtained after the experiment was performed. The fineness modulus obtained from the

sieve analysis was 6.8% which falls within the range (5.5 % - 8.0%) for coarse aggregates. The result was obtained in this research was higher than that obtained by Odeyemi *et al.* (2021) when they determined the grain size for granite used in the design of their concrete. This is because the granite used for this research is coarser than that reported by the authors. Figure 3 also confirms the size of the granite particles used in this research as the grain diameter were found to between 3.6 mm to 20 mm with most grains falling in the coarse range of particle distribution.

Table 3 Sieve analysis of coarse aggregate

Sieve Sizes(mm)	Wt. retained (g)	% Wt. retained	Cumulative % Wt. retained	% Passing
20.0	0.0	0.0	0.0	100.0
10.0	1670.5	83.5	83.5	16.5
6.25	327.5	16.4	99.9	0.1
2.36	0.0	0.0	99.9	0.1
1.18	0.0	0.0	99.9	0.1
0.6	0.0	0.0	99.9	0.1
0.3	0.0	0.0	99.9	0.1
0.15	0.0	0.0	99.9	0.1
Total Cumulative % Wt. retained			682.9	
Pan	2.0	0.1	100.0	0.0

3.1.4 Specific gravity (S.G.) of materials

The S.G. of Cement, sharp sand and granite used in this study was obtained as 3.11, 2.57 and 2.69 respectively. It was observed that the S.G. of cement obtained in this research was like that obtained by Tijani *et al.* (2020) while the S.G. of the granite was the same with that reported by Odeyemi *et al.* (2020). Also, the specific gravity of the sharp sand fell in the range (2.5-3.0) stated for natural aggregates by Neville (2011).

3.1.5 Normal Consistency, soundness and setting time of cement

The result of the normal consistency of cement was obtained as 32%. There was no reaction between water and cement when the quantity of water added was less than the standard consistency. The soundness of ordinary Portland cement was found to be 1mm. According to BS EN 196-3: (2016), soundness for ordinary Portland cement must not exceed 10mm. Therefore, since the result obtained was 1 mm then the result indicates that the cement can still

maintain its volume after it gets hardened. The initial and final settling time of the cement used in this study was found to be 1 hour 3 minutes and 6 hours 8 minutes respectively. The temperature of the cement, water, and room were all 29 ^{o}C.

3.1.6 Water Absorption Capacity of Sharp Sand and Granite

The water absorption capacity for sharp sand and granite were found to be 1.4 % and 0.2 % respectively. This indicates that the sharp sand has larger absorption capacity than the granite. It also indicates that the sharp sand has more pores for absorption and could retain more water than the granite.

3.1.7 Aggregate Crushing Value

Aggregate crushing value was found to be 21.5 %. This indicates that the resistance to the applied compressive load by the aggregate is high. Jethro *et al*. (2013) obtained a coarse aggregate value of 21.6 % for granite and concluded that the resistance of granite is highly durable for engineering work and road construction.

3.1.8 Alkalinity of water

The pH of the water used was found to be 7.5. This indicated that the water is neutral. If it is too acidic or basic, it may attack the concrete by dissolving both hydrated and unhydrated cement compounds or even react with the compounds present in the carbonated guinea corn husk ash, thereby causing shrinkage in the concrete.

3.2 Flow Parameters

The responses of the flowability parameters (Slump flow test T50 (sec), slump flow test (mm), L-Box and the V-funnel) for the experimental design are presented in Table 4. Figure 4 displays the variation of cement and GCHA with the slump flow test T50. It revealed that as the quantity cement increases the slump flow also increases. Nevertheless, with the increase in GCHA content, the slump flow reduced. Figure 5 shows the variation of cement and GCHA with the slump. It revealed that as the proportion of cement increases the slump flow also increases until it peaked at about 435 kg/m^3 before declining. However, with the rise in GCHA content, the slump flow increases significantly. Figure 6 shows the variation of cement and GCHA with the V-funnel flow. It revealed that as the proportion of cement increases the V-funnel flow equally increases. But, with the increase in GCHA content, the V-funnel flow decreases.

Figure 7 shows the variation of cement and GCHA with L-box. It revealed that as the proportion of cement increases the L-box increases until it peaked at about 435 kg/m^3 before declining. However, with the increase in GCHA content, the L-box increases.

3.3 Compressive Strength Result for the SCC

The compressive strength of the cubes was gotten after 7, 28 and 56 days of curing respectively for both accelerated curing and water curing methods. Figure 8(a) and Figure 8(b) shows the 3D diagram of a quadratic model for compressive strength at 7 days for ACC and WC respectively. It was observed that for both curing methods, the compressive strengths rose in magnitude with the increase in the proportion of both cement and GCHA. The same trend, as noted in the result obtained at 7 days, was observed for both curing methods at 28 and 56 days of testing as depicted in Figures 9 and 10 respectively.

Table 4 The Flowability Responses Parameter

Runs	Slump flow T50(mm)	Slump flow (mm)	V-Funnel (secs)	L-Box		
				H_2 (mm)	H_1 (mm)	H_2/H_1
1	4	725	5	80	95	0.84
2	4	710	5	75	90	0.83
3	5	685	6	70	85	0.82
4	4	725	5	80	90	0.84
5	6	650	7	50	60	0.83
6	3	800	4	90	100	0.9
7	7	650	8	90	110	0.82
8	4	730	5	75	90	0.83
9	4	725	5	80	95	0.84
10	4	725	5	80	95	0.84
11	4	750	5	85	100	0.85
12	4	725	5	80	95	0.84
13	5	680	6	60	70	0.86

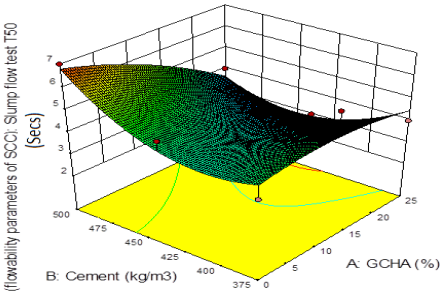


Figure 4: Variation of cement and GCHA with Slump Flow T50

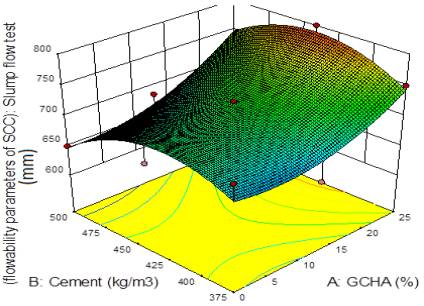


Figure 5: Variation of cement and GCHA with Slump Flow

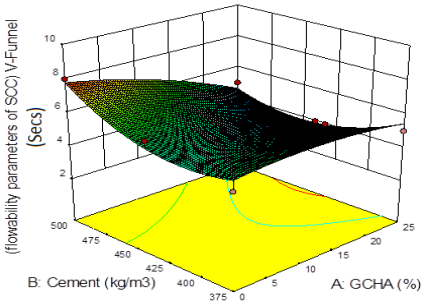


Figure 6: Variation of cement and GCHA with V-Funnel

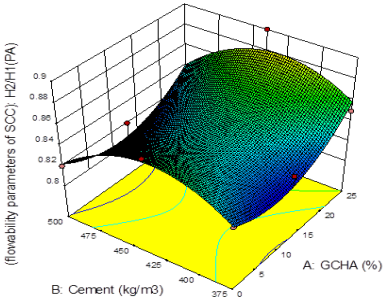
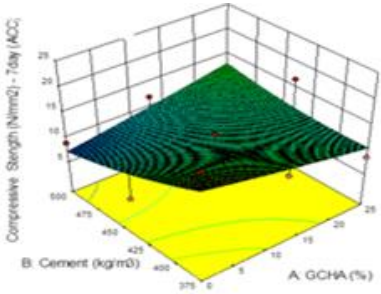
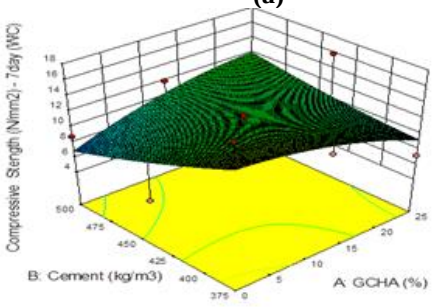


Figure 7: Variation of cement and GCHA with L-Box



(a)



(b)

Figure 8: Compressive strength at 7 days (a) ACC (b) WC

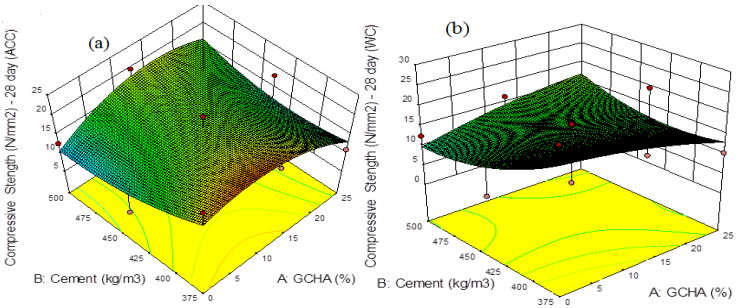


Figure 9: Compressive strength at 28 days (a) ACC (b) WC

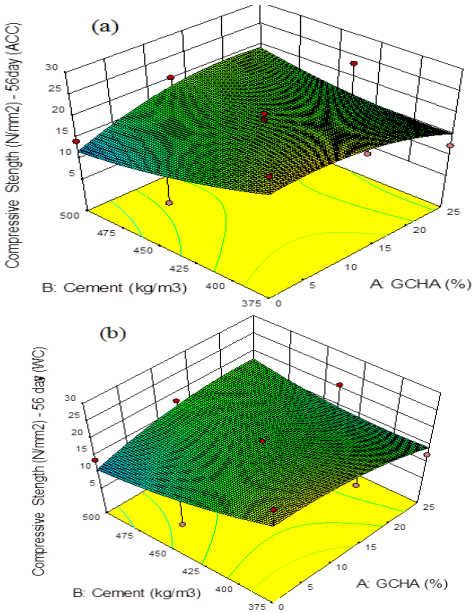


Figure 10: Compressive strength at 56 days (a) ACC (b) WC

3.4 Optimization of materials

To optimize the combination ratio, the objective was to maximize the compressive strength of the concrete and the percentage proportion of GCHA while that of cement was minimized.

It was discovered that the optimum combination of percentage of GCHA and cement that gave a compressive strength of 21.369 N/mm^2 (Figure 11b) in 56 days are 25 % and 412.5 kg/m^3 of cement respectively. This is greater than the target compressive strength of 20 N/mm^2. Also, the flow parameters at this optimum combination were found to be 5mm for Slump flow test T50 (sec) ,690 mm for slump flow test (mm), 0.88 for L-Box and 6secs for V-funnel. The mathematical model that relates the compressive strength to the percentage of GCHA and the quantity of cement is presented as Equation 11. This model has a *p*-value of 0.0471, signifying that it is significant. This result has a combined desirability value of 0.799 as presented in Figure 11a.

Compressive Strength (N/mm^2) [56 days ACC] =

$$= 18.65 + 0.25\ x\ A\ -1.45\ x\ B\ + 3.52\ x\ AB\ –2.82\ x\ A^2\ +1.28\ x\ B^2 \qquad (11)$$

Where A = GCHA %, B = Cement kg/m^3

Similarly, for concrete samples cured by immersion in water, it was discovered that the optimum combination of percentage of GCHA and cement that gave a compressive strength of 19.6274 N/mm^2 (Figure 12b) in 56 days are 25 % and 412.5 kg/m^3 of cement. This strength is lower than the one obtained when the concrete was cured using ACC method. However, this combination still gave a strength that is equivalent to the target strength of 20 N/mm^2. The model that relates the compressive strength to the percentage of GCHA and the quantity of cement is presented as Equation 12. The *p*-value of this model is 0.0085, indicating that it is significant. This result also has a combined desirability value of 0.769 as presented in Figure 12a.

Compressive Strength (N/mm^2) [56 days WC] =

$$= 16.88 – 0.100\ x\ A\ -1.88\ x\ B\ +3.63\ x\ AB\ – 2.07\ x\ A^2\ +1.58\ x\ B^2 \qquad (12)$$

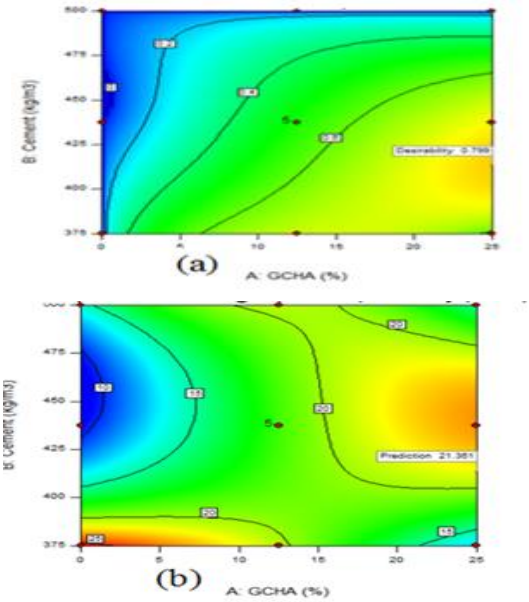


Figure 11: Optimized results for GCHA blended SCC (a) desirability value (b) predicted strength

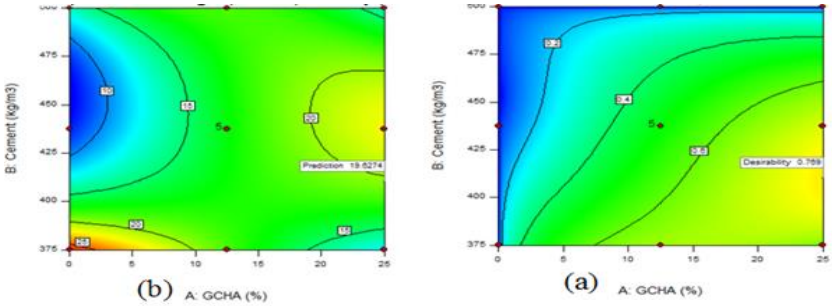
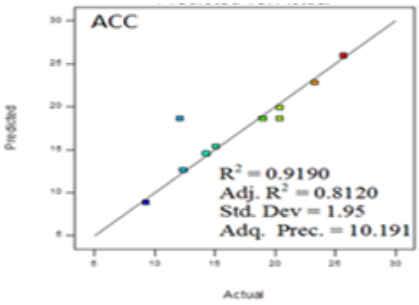


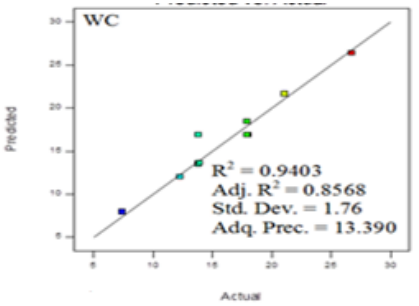
Figure 12: Optimized results for GCHA blended SCC (a) desirability value (b) predicted strength

3.5 Validation of Results for ACC and WC

The predicted versus the actual result for the compressive strength for ACC and WC is shown in Figure 13. The figure revealed that both the predicted and actual data are close. The R^2 value of 0.9190 and an adjusted R^2 value of 0.8120 and R^2 value of 0.9403 and an adjusted R^2 value of 0.8569 for ACC and WC respectively also validate the results obtained. The adequate precision ratio of 10.191 and 13.390 for ACC and WC respectively is greater than 4. This indicates that the model is adequate to move through the design space



(a)



(b)

Figure 13: Predicted versus the actual data
(a) ACC cured concrete;
(b) WC cured concrete

3.6 Durability Test

3.6.4 Coefficient of Water Absorption

Figure 14 displays the plot of water absorption against the age for curing for ACC and WC. It reveals that as the curing days increases the water absorption also increases. This suggests that the total reachable pore volume of the concrete becomes more exposed as the curing day increases. In general, the absorption water value of concrete cured by ACC is more than that of concrete cured by WC.

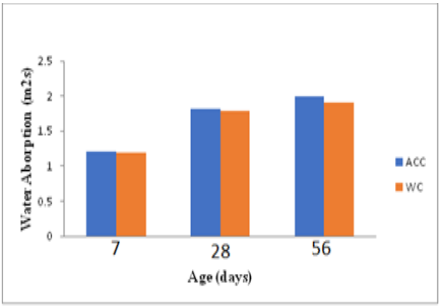


Figure 14: The water absorption test for self-compacting concrete.

3.6.5 Sorptivity Test

The highest value of sorptivity occurred in ACC. This indicates that pore structure and connectivity are better exposed compared to that of WC.

3.7 Characterization of Calcined GCHA

3.7.4 XRD Analysis of Calcined GCHA

The X-ray diffraction pattern of the calcined GCHA is presented in Figure 15. It shows the presence of a crystalline compound in the calcined GCHA. The peaks according to the joint committee powder diffraction standard (JCPDS card: #850335), at 2 theta (2θ) angles 20.2008°, 28.2348°, 41.0028°, 43.564°, 54.6025°, and 61.9344° are attributed to the presence of SiO_2 (Quartz) particles. The material (GCHA) formed a hexagonal crystalline structure. A similar result was reported by Nandanwar *et al.* (2015) when they characterized SiO_2 nanoparticles developed by sol-gel process and obtained a hexagonal shape.

3.7.5 XRF Analysis of Calcined GCHA

Table 5 shows the oxides composition of the GCHA used in this study. The result showed that that the oxide of the GCHA mainly contains SiO_2 (63.1559%), K_2O (23.4164%), Al_2O_3 (4.1534%), MgO (3.3649%), Fe_2O_3 (4.6572%). It was determined that the summation of the oxides Al_2O_3, SiO_2, and Fe_2O_3 which gave 71.9665% is above the threshold of 70 % stated for supplementary cementitious materials by ASTM C618 (2019). This result agrees with what was obtained by Odeyemi *et al.* (2020a) and Ndububa and Nurudeen (2015). This is also similar to what was obtained by Odeyemi *et al.* (2022) for a bamboo leaf ash (BLA). These further confirms that the GCHA is suitable as a pozzolan in concrete.

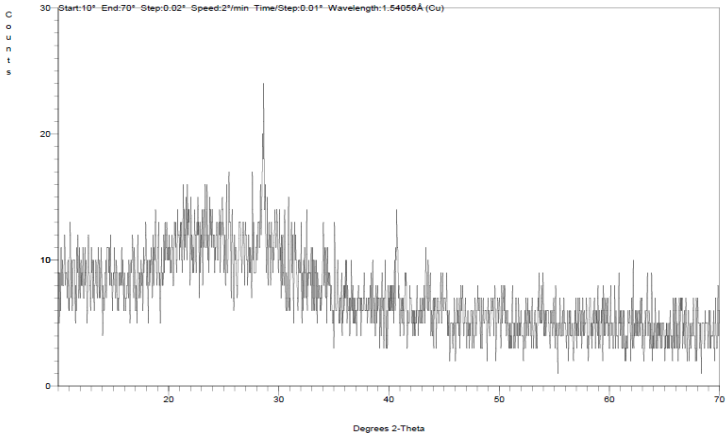


Figure 15: The XRD pattern of the calcined GCHA

Table 5 The oxide composition of calcined GCHA

OXIDE CONVERSION	GCHA OXIDE %
MgO	3.3649
Al_2O_3	4.1534
SiO_2	63.1559
P_2O_5	2.2621
SO_3	4.0899
K_2O	23.4164
CaO	6.9492
TiO_2	0.0000

V_2O_5	0.0000
Cr_2O_3	0.0000
MnO	0.0187
CoO	0.0000
Fe_2O_3	4.6572
NiO	0.0098
CuO	0.0483
ZnO	0.2338
As_2O_3	0.0049
PbO_2	0.0559
WO_3	0.3297
Au_2O	0.0000
Ag_2O	0.0018
Rb_2O	0.0489
Nb_2O_5	0.0062
MoO_3	0.3045
CdO	0.000
SnO_2	0.4802
Sb_2O_3	0.4169
*LOI	-

* Loss on Ignition

3.8 SEM Analysis of Calcined GCHA

The morphological structure of the GCHA after calcination at 650 ℃ is presented in Figure 16. Figure 16(a-d) are of the same width of 15.8 mm but different magnifications. Figure 16a shows the image of the GCHA at display magnification of 250.The structure contains several pores of irregular size. A closer look at the display in Figure 17b showed that the GCHA (at magnification of 500) also contains flat- like materials with rough edges. Moreover, at Figure 17(c-d) (magnification of 750 and 1000 respectively), it could be seen clearly that there are alternating pattern of arrangement on the GHCA image that are well compacted.

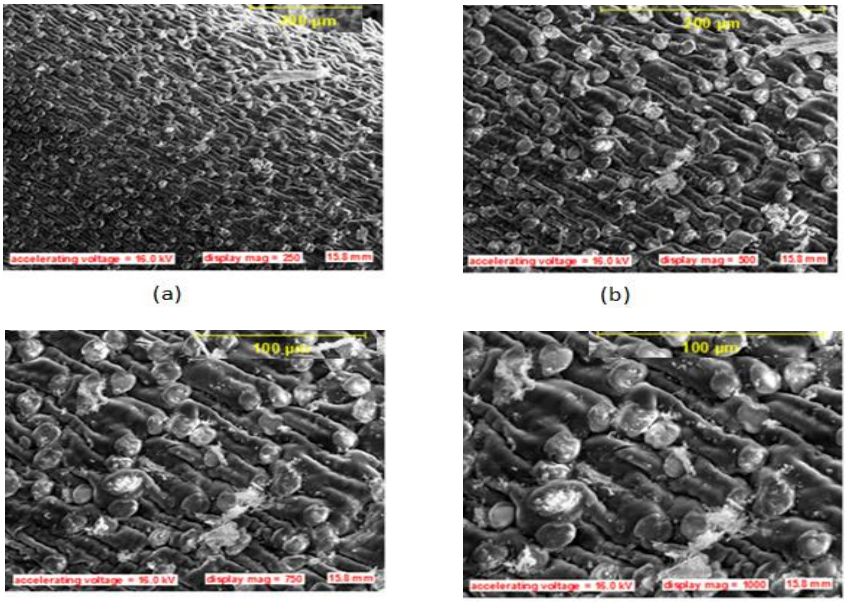


Figure 16: The SEM Image of calcined CGHA at different Magnification (a) 250 (b) 500 (c) 750 (d) 1000

4 Conclusion

This study was based on determining the mechanical and durability properties of GCHA blended SCC. The optimum flowability parameters such as slump flow, slump flow T_{50}, L-Box test, and V-funnel test were determined using the CCD. Having carried out this research, it was be concluded that:

(a) The chemical composition and morphology of the GCHA shows that it is a pozzolan.

(b) The optimum combinations of percentage of GCHA and cement cured by ACC that will give a compressive strength of 21.369 N/mm^2 in 56 days are 25 % and 412.5 kg/m^3 of cement. Also, the optimum combination of percentage of GCHA and cement for WC that will give a compressive strength of 19.6274 N/mm^2 in 56 days are 25 % and 412.5 kg/m^3 of cement.

(c) The compressive strength of concrete samples developed after being cured by ACC and WC methods were equivalent to the target strength of 20 N/mm^2.
(d) As the curing days increases the coefficient of water absorption also increases for both ACC and WC. However, the highest value of sorptivity occurred in ACC which indicates that the pore structures are more exposed than that of WC.

References

Adeyanju, E., & Okeke, C. A. (2019). Exposure effect to cement dust pollution: a mini review. *SN Applied Sciences*, *1*(12), 1–17. https://doi.org/10.1007/s42452-019-1583-0

Aggarwal, P., Siddique, R., Aggarwal, Y., & Gupta, S. M. (2008). Self-compacting concrete - Procedure for mix design. *Leonardo Electronic Journal of Practices and Technologies*, *7*(12), 15–24.

Akinpelu, M. A., Odeyemi, S. O., Olafusi, O. S., & Muhammed, F. Z. (2019). Evaluation of splitting tensile and compressive strength relationship of self-compacting concrete. *Journal of King Saud University – Engineering Sciences*, *31*, 19–25. https://doi.org/http://dx.doi.org/10.1016/j.jksues.2017.01.002

Assaggaf, R. A., Adekunle, S. K., Ahmad, S., Maslehuddin, M., Al-Amoudi, O. S. B., & Ali, S. I. (2019). Mechanical properties, durability characteristics and shrinkage of plain cement and fly ash concretes subjected to accelerated carbonation curing. *Journal of the South African Institution of Civil Engineering*, *61*(4), 73–81. https://doi.org/10.17159/2309-8775/2019/v61n4a7

ASTM C618. *Standard Specification for Coal Fly Ash and Raw or Calcined Natural Pozzolan for Use in Concrete, ASTM International, West Conshohocken, PA, 2019.* , (2019).

Bello, M. O., Abdus-Salam, N., & Adekola, F. A. (2018). Utilization of Guinea corn (Sughurm vulgare) Husk for Preparation of Bio-based Silica and it's Characterization Studies. *International Journal of Environment, Agriculture and Biotechnology*, *3*(2), 670–675.

https://doi.org/10.22161/ijeab/3.2.48

Bhagat, D. K., Dawda, N. H., Goyal, D. L., Navneet, T., & Panchal, U. N. (2014). Designing Concrete Of New Era: "Self Compacting Concrete." *International Journal of Engineering Research and Applications*, *4*(2), 36–39. https://doi.org/10.13140/RG.2.2.14083.30241

BS 1377-3:2018+A1:2021. (2018). *Methods of test for soils for civil engineering purposes - Chemical and electro-chemical testing*.

BS EN 12390-3. (2019). *Testing hardened concrete. Compressive strength of test specimens*.

BS EN 12620:2002+A1:2008. (2008). *Specification for Aggregates from natural sources for concrete. British Standards, BSI Group Headquarters 389 Chiswick High Road, London, W4 4AL, UK, Standards Policy and Strategy Committee.*

BS EN 196-3, B. (2016). *Methods of testing cement part 3: Determination of setting times and soundness*.

BS EN 933-1. (2012). *Tests for Geometrical Properties of Aggregates - Part 1: Determination of Particle Size Distribution - Sieving Method*.

BS ISO 3310-2. (2013). *Test sieves. Technical requirements and testing - Test sieves of perforated metal plate*.

Ehikhuenmen, S. O., Igba, U. T., Balogun, O. O., & Oyebisi, S. O. (2019). The influence of cement fineness on the structural characteristics of normal concrete. *IOP Conference Series: Materials Science and Engineering*, *640*(1). https://doi.org/10.1088/1757-899X/640/1/012043

Fapohunda, C. A., Famodimu, B. I., Adigo, B. C., & Jeje, A. S. (2020). Comparative Study of Durability and Microstructure Properties of Concrete made with Different Grades of Nigerian Portland Limestone Cement. *ARID ZONE Journal of Engineering, Technology & Environment*, *16*(3), 569–578.

Fapohunda, C., Bello, H., Salako, T., & Tijani, S. (2020). Strength, Micro-Structure & Durability Investigations of Lateritic Concrete with Palm Kernel Shell (PKS) as Partial Replacement of Coarse Aggregates. *Engineering*

Review, *40*(2), 59–69.

He, P., Shi, C., Tu, Z., Poon, C., & Zhang, J. (2016). Effect of further water curing on compressive strength and microstructure of CO2-cured concrete. *Cement and Concrete Composites*, *72*, 80–88. https://doi.org/https://doi.org/10.1016/j.cemconcomp.2016.05.026

Jethro, M. A., Shehu, S. A., & Olaleye, B. M. (2013). The Suitability of Some Selected Granite Deposits for Aggregate Stone Production in Road Construction. *The International Journal Of Engineering And Science (IJES)*, *3*(2), 75–81.

Kashani, A., & Ngo, T. (2020). Production and placement of self-compacting concrete. In *Self-Compacting Concrete: Materials, Properties and Applications* (pp. 65–81). Woodhead Publishing Series in Civil and Structural Engineering.

McCarthy, M. J., & Dyer, T. D. (2019). Pozzolanas and Pozzolanic Materials. In *Lea's Chemistry of Cement and Concrete (Fifth Edition)* (pp. 363–467).

Nandanwar, R., Singh, P., & Fozia, Z. H. (2015). Synthesis and characterization of SiO2 Nanoparticles by Sol-Gel Process and its Degradation. *American Chemical Science Journal*, *5*(1), 1–10.

Ndububa, E., & Yakubu, N. (2015). Effect of Guinea Corn Husk Ash as Partial Replacement for Cement in Concrete. *IOSR Journal of Mechanical and Civil Engineering*, *12*(2), 40–45. https://doi.org/10.9790/1684-12214045
Neville, A. M. (2011). *Properties of Concrete* (5th ed.). Pearson Education Ltd.

Odeyemi, S. O., Anifowose, M. A., Abdulwahab, R., & Oduoye, W. O. (2020). Mechanical Properties of High-Performance Concrete with Guinea Corn Husk Ash as Additive. *LAUTECH Journal of Civil and Environmental Studies*, *5*(September 2020), 139–154. https://doi.org/10.36108/laujoces/0202/50(0131)

Odeyemi, S. O., Atoyebi, O. D., & Ayo, E. (2020a). Effect of Guinea Corn Husk Ash on the Mechanical Properties of Lateritic Concrete Effect of Guinea Corn Husk Ash on the Mechanical Properties of Lateritic Concrete.

IOP Conference Series. https://doi.org/10.1088/1755-1315/445/1/012034

Odeyemi, S. O., Atoyebi, O. D., & Ayo, E. K. (2020b). Effect of Guinea Corn Husk Ash on the Mechanical Properties of Lateritic Concrete. *IOP Conference Series: Earth and Environmental Science*, *445*(012034), 1–11. https://doi.org/10.1088/1755-1315/445/1/012034

Odeyemi, S. O., Atoyebi, O. D., Kegbeyale, O. S., Anifowose, M. A., Odeyemi, O. T., Adeniyi, A. G., & Orisadare, O. A. (2022). Mechanical properties and microstructure of High-Performance Concrete with bamboo leaf ash as additive. *Cleaner Engineering and Technology*, *6*, 1–6. https://doi.org/10.1016/j.clet.2021.100352

Pathak, N., & Siddique, R. (2012). Properties of self-compacting-concrete containing fly ash subjected to elevated temperatures. *Construction and Building Materials*, *30*, 274–280. https://doi.org/https://doi.org/10.1016/j.conbuildmat.2011.11.010

Su, N., Hsu, K., & Chai, H. (2001). A simple mix design method for self-compacting concrete. *Cement and Concrete Research*, *31*(12), 1799–1807.

Tijani, M. A., Ajagbe, W. C., Ganiyu, A. A., Aremu, A. S., & Ojewole, Y. N. (2020). Strength and Absorption of Sorghum Husk Ash Sandcrete Blocks. *Premier Journal of Engineering and Applied Science*, *1*(1), 1–7.